

SCIENTIFIC REPORTS



OPEN

Blockade of microglial adenosine A_{2A} receptor impacts inflammatory mechanisms, reduces ARPE-19 cell dysfunction and prevents photoreceptor loss *in vitro*

M. H. Madeira ^{1,2,3}, K. Rashid³, A. F. Ambrósio ^{1,2,4}, A. R. Santiago ^{1,2,4} & T. Langmann ³

Age-related macular degeneration (AMD) is characterized by pathological changes in the retinal pigment epithelium (RPE) and loss of photoreceptors. Growing evidence has demonstrated that reactive microglial cells trigger RPE dysfunction and loss of photoreceptors, and inflammasome pathways and complement activation contribute to AMD pathogenesis. We and others have previously shown that adenosine A_{2A} receptor (A_{2A}R) blockade prevents microglia-mediated neuroinflammatory processes and mediates protection to the retina. However, it is still unknown whether blocking A_{2A}R in microglia protects against the pathological features of AMD. Herein, we show that an A_{2A}R antagonist, SCH58261, prevents the upregulation of the expression of pro-inflammatory mediators and the alterations in the complement system triggered by an inflammatory challenge in human microglial cells. Furthermore, blockade of A_{2A}R in microglia decreases the inflammatory response, as well as complement and inflammasome activation, in ARPE-19 cells exposed to conditioned medium of activated microglia. Finally, we also show that blocking A_{2A}R in human microglia increases the clearance of apoptotic photoreceptors. This study opens the possibility of using selective A_{2A}R antagonists in therapy for AMD, by modulating the interplay between microglia, RPE and photoreceptors.

Age-related macular degeneration (AMD) is a major cause of vision loss worldwide and the leading cause of blindness in the elderly in developed countries¹. The accumulation of cellular debris as drusen in the subretinal space, beneath the retinal pigment epithelium (RPE), is a main feature of early and intermediate AMD, which can progress to photoreceptor loss, representing the so-called dry AMD. Wet AMD is characterized by choroidal neovascularization, with new blood vessels arising from the choroid through the RPE layer into the outer retina, leading to photoreceptor dysfunction².

Growing evidence supports a critical role of the immune system in AMD^{3,4}. Recruitment of microglial cells, the immunocompetent cells of the central nervous system (CNS), has been associated with the progression and severity of AMD^{5,6}. Indeed, microglia reactivity is involved in the recruitment and activation of complement system^{7,8} and inflammasome pathways⁹, which may contribute to photoreceptor degeneration¹⁰.

The complement system and inflammasome pathways, key innate immune defenses against inflammation, orchestrate critical responses in the CNS. Several studies reported the involvement of the complement cascades in both acute and chronic disease conditions^{11,12}. Genetic variations of several complement-related genes are associated with AMD pathogenesis^{13–16}. Similarly, elevated levels of complement factors have been detected in the plasma and aqueous humor of AMD patients^{17,18}. Moreover, complement proteins are present in drusen. Notably, A2E, a RPE lipofuscin and drusen component, triggers microglia reactivity and complement activation

¹Institute for Biomedical Imaging and Life Sciences (IBILI), Faculty of Medicine, University of Coimbra, Coimbra, Portugal. ²CNC.IBILI Consortium, University of Coimbra, Coimbra, Portugal. ³Laboratory for Experimental Immunology of the Eye, Department of Ophthalmology, University of Cologne, Cologne, Germany. ⁴Association for Innovation and Biomedical Research on Light and Image (AIBILI), Coimbra, Portugal. Correspondence and requests for materials should be addressed to T.L. (email: thomas.langmann@uk-koeln.de)

by increasing complement factor B (CFB) and decreasing complement factor H (CFH) expression, leading to photoreceptor degeneration⁸.

Inflammasome is a large multiprotein complex that takes part in the innate immune response, promoting interleukin 1 β (IL-1 β) and interleukin 18 (IL-18) maturation, through caspase-1-mediated cell death, known as pyroptosis¹⁹. AMD-associated inflammasome activation has been widely described. There is evidence showing the ability of drusen to induce the activation of inflammasome, namely NLRP3 inflammasome, in retinal mononuclear cells²⁰. Inflammasome has been detected in the RPE, in both dry and wet AMD, and might contribute to RPE degeneration^{21,22}. Interestingly, factors released from reactive microglia can also induce the activation of NLRP3 inflammasome in ARPE-19 cells⁹.

Adenosine is a crucial neuromodulator in the CNS, and blockade of adenosine A_{2A} receptor (A_{2A}R) affords robust neuroprotection against different neurodegenerative conditions²³. We have recently reported that A_{2A}R blockade prevents retinal microglia reactivity and the associated neuroinflammatory response, conferring protection to retinal ganglion cells, in experimental models of glaucoma^{24–26}. Still, the impact of A_{2A}R modulation on the complement system and its potential beneficial effects on AMD remain to be elucidated.

Hence, the main aim of this work was to evaluate the outcome of A_{2A}R blockade in the microglial complement system. Moreover, we evaluated the potential beneficial effects of blocking A_{2A}R in human microglial cells on the inflammatory response of ARPE-19 cells, inflammasome activation and photoreceptor loss.

Results

Inflammatory stimuli increase the release of adenosine and the density of A_{2A}R in human microglial cells. It is well known that A_{2A}R is up-regulated under noxious conditions^{24,25,27}. Therefore, we firstly investigated whether the incubation of human microglial cells with Zymosan and phorbol myristate acetate (PMA), two potent pro-inflammatory stimuli²⁸, would be able to increase the levels of extracellular adenosine, which then could boost A_{2A}R activation, and affect A_{2A}R expression.

In control conditions, the concentration of extracellular adenosine was 308 ± 152 pmol/μL (n = 7). The incubation with Zymosan + PMA for 6 h or 24 h increased the concentration of adenosine to 593.7 ± 205.4 or 941.1 ± 205 pmol/μL, respectively (n = 4–7; Fig. 1A). Also, A_{2A}R mRNA expression was significantly up-regulated (1.3-fold increase, n = 5) after 6 h incubation with Zymosan + PMA when compared with the control condition (Fig. 1B). Moreover, the incubation of human microglia with Zymosan + PMA for 6 h or 24 h increased the immunoreactivity of A_{2A}R (159 ± 12.1 and 128.6 ± 8.7% of control, respectively; n = 4; Fig. 1C and D). These results demonstrate that pro-inflammatory conditions can trigger an increase in the release of adenosine from human microglia that may then signal through the upregulated A_{2A}R.

Treatment with an A_{2A}R antagonist reduces the inflammatory response in human microglia. Considering that A_{2A}R expression and density increased in human microglia exposed to Zymosan + PMA and that a selective antagonist of A_{2A}R prevented the neuroinflammatory response²⁴, we next investigated whether A_{2A}R blockade could influence human microglia reactivity.

The incubation of human microglia with Zymosan + PMA for 6 h up-regulated the mRNA expression of the inflammatory markers CCL2, TNF and IL-8 (n = 7). Pre-treatment with 50 nM SCH58261, the A_{2A}R antagonist, reduced the stimulatory effect of Zymosan + PMA (n = 7; Fig. 2A–C). SCH58261 by itself did not alter the expression of these pro-inflammatory markers.

The incubation of microglia with Zymosan + PMA for 6 h or 24 h also increased the release of NO by human microglia, as determined by the nitrite concentration in culture supernatants (223.9 ± 37.1 and 298.3 ± 63.3% of control, respectively, n = 6–8). The blockade of A_{2A}R prevented the increase in NO induced by Zymosan + PMA (118.7 ± 12.3 and 116.8 ± 20.8% of control for 6 h and 24 h, respectively) (Fig. 2D).

Since reactive microglia are characterized by the ability to phagocytose foreign material, we determined the phagocytic efficiency of human microglia following exposure to Zymosan + PMA, in the absence or presence of the A_{2A}R antagonist. The incubation of human microglia with Zymosan + PMA significantly increased the number of phagocytosed polystyrene microparticles (206.9 ± 36% of control, n = 5). This effect was partially reduced by the pre-treatment with SCH58261 (138 ± 20.6% of control, n = 5). Taken together, these results indicate that A_{2A}R blockade prevents the shift of human microglia into a reactive phenotype.

Blockade of A_{2A}R prevents the upregulation of complement components in human microglia induced by Zymosan + PMA. Complement system modulation is an emerging therapeutic strategy for AMD²⁹. Although A_{2A}R blockade controls microglia reactivity²³, the direct effects of A_{2A}R blockade on the complement system of microglia are unknown. Hence, we addressed this question in human immortalized microglial cells to evaluate whether the A_{2A}R antagonist could modulate the expression of complement factor in microglial cells.

Incubation of human microglia with Zymosan + PMA for 6 h increased the expression of complement components associated with the activation of the cascade: complement C3 (Fig. 3A), CFB (Fig. 3B), CD91 (also known as C1qr; Fig. 3C), and complement C5a receptor 1 (C5AR1) (Fig. 3D). When the cells were pre-treated with the A_{2A}R selective antagonist, the upregulation of these components was prevented. Concerning the inhibitory complement components, Zymosan + PMA decreased CFH (Fig. 3E), CFI (Fig. 3F), CD46 (also known as MCP; Fig. 3G), and CD55 (also known as DAF; Fig. 3H), and these inhibitory effects were absent in the presence of the A_{2A}R antagonist. No alterations were observed in the mRNA levels of C1s (Fig. 3I). Treatment of human microglia with SCH58261 did not change the expression of complement components.

A_{2A}R blockade prevents microglia reactivity induced by exposure to ARPE-19 debris. Drusen components can induce microglia reactivity and complement activation⁸. Therefore, we evaluated whether A_{2A}R

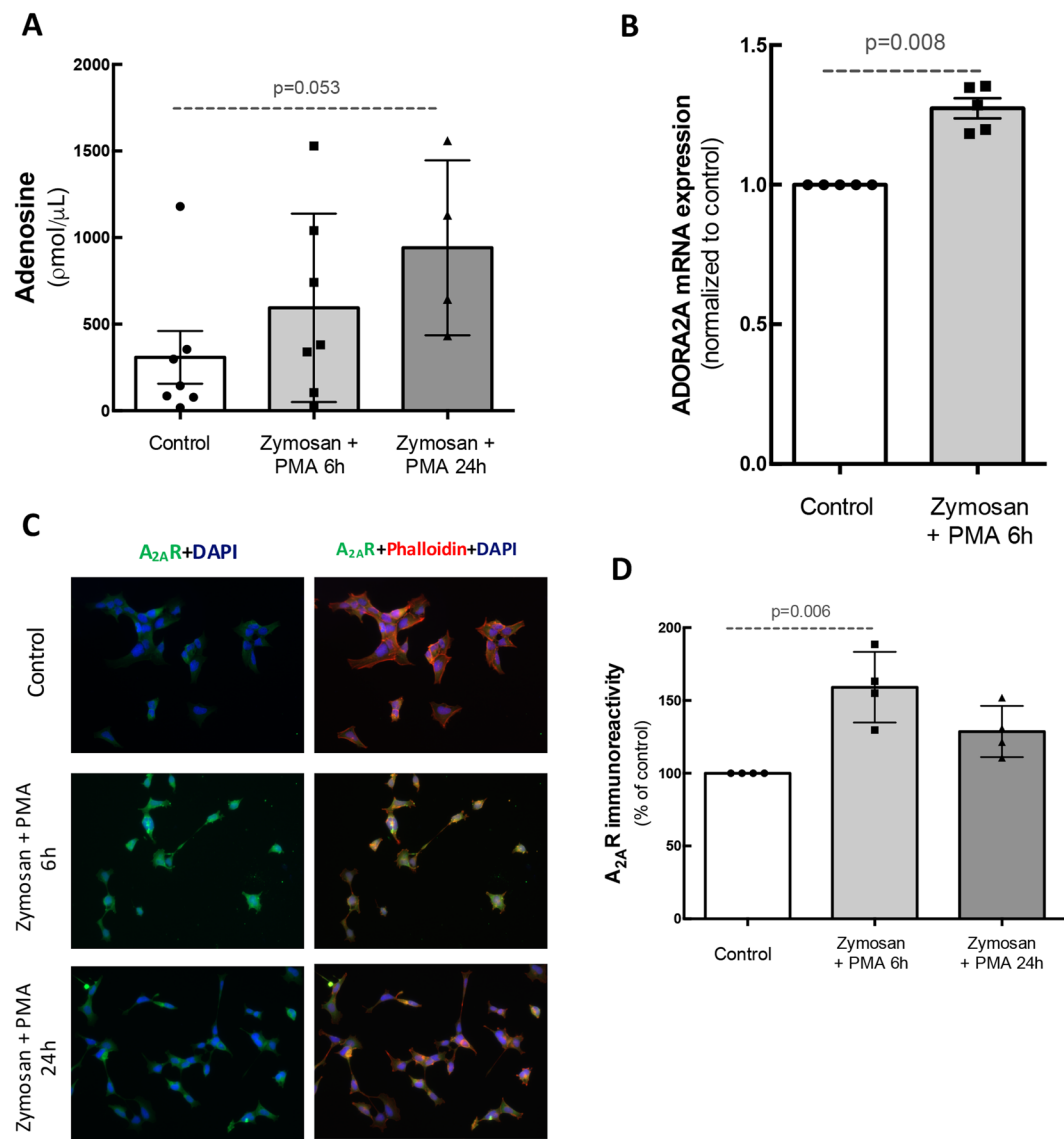


Figure 1. Inflammatory stimulus increases the release of adenosine and the expression and density of A_{2A}R in human microglia. Human immortalized microglial cells were challenged with Zymosan + PMA for 6 h or 24 h. **(A)** Adenosine concentration in culture supernatants. Data are expressed as percentage of control and represent the mean \pm SEM of 3–7 independent experiments (presented with the scatterplot with the individual data points). **(B)** The mRNA levels of A_{2A}R were assessed by qPCR relatively to *hprt* (housekeeping gene). Results are normalized to control from 3–7 independent experiments. Mann-Whitney test. **(C)** Microglial cells (red; phalloidin) were immunostained for A_{2A}R (green). Nuclei were stained with DAPI (blue). Images are representative of 4–7 independent experiments. **(D)** Densitometric analysis of A_{2A}R immunoreactivity. Data represent the mean \pm SEM, with the scatterplot with the individual data points. Results are expressed as percentage of control and were obtained from 4–7 independent experiments. Kruskal-Wallis test, followed by Dunn's multiple comparison test.

blockade could prevent the reactivity of human microglia induced by RPE debris, which were used to mimic drusen components.

We first evaluated the ability of different concentrations and times of exposure of ARPE-19 debris to induce an inflammatory response in microglial cells (Sup. Figure 1). All challenges with ARPE-19 cell debris induced up-regulation of CCL2 and IL-8 mRNA expression, but not TNF. We choose 5 μ g/ μ L ARPE-19 cell debris since it was the shorter time point and lower concentration.

Then, human microglial cells were challenged with RPE debris (5 μ g/ μ L of ARPE-19 cell debris for 6 h) 45 minutes after incubation with A_{2A}R antagonist. The A_{2A}R antagonist partially prevented the increase in the mRNA expression of CCL2 (Fig. 4A) and IL-8 (Fig. 4B). The mRNA expression levels of TNF were not altered by ARPE-19 cell debris in the absence or presence of SCH58261 (Fig. 4C).

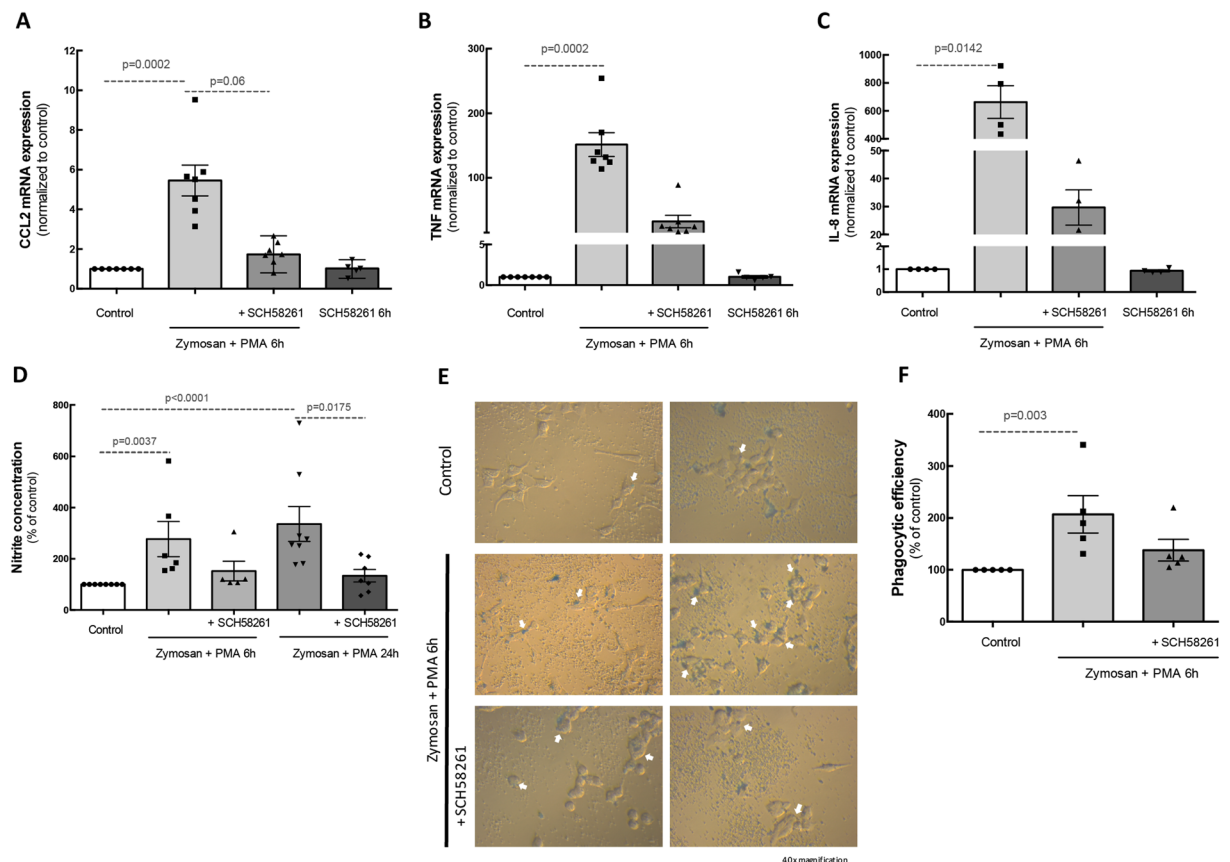


Figure 2. $A_{2A}R$ blockade reduces the inflammatory response in human microglia. Human microglial cells were challenged with Zymosan + PMA in the absence or presence of 50 nM SCH58261. The mRNA levels of CCL2 (A), TNF (B) and IL-8 (C) were assessed by qPCR. Results are normalized to control from 5–7 independent experiments. (D) The release of NO was assessed by the Griess reaction assay in culture supernatants. Results are expressed in percentage of control and presented as the mean \pm SEM of 4–7 independent experiments (the individual data points for each condition are also presented). (E) Human microglial cells were incubated with Zymosan + PMA for 2 h in the absence or presence of SCH58261, before adding polystyrene beads for 6 h (white arrows). Images were acquired and the phagocytic efficiency was determined (F). Results are expressed as percentage of control and presented as the mean \pm SEM of 5 independent experiments (the individual data points for each condition are also presented). Kruskal-Wallis test, followed by Dunn's multiple comparison test.

$A_{2A}R$ blockade prevents changes in complement components in microglia induced by exposure to ARPE-19 debris.

We then evaluated whether the ARPE-19 cell debris were able to induce alterations in the expression of complement components of human microglia. When human microglia were incubated for 6 h with ARPE-19 cell debris the mRNA expression of C3 (Fig. 5A; $n = 5$), CFB (Fig. 5B; $n = 5$) and C5AR1 (Fig. 5C; $n = 5$) increased and this effect was prevented by the blockade of $A_{2A}R$. The transcript levels of the inhibitory components CFH (Fig. 5D), CFI (Fig. 5E), CD46 (Fig. 5F) and CD55 (Fig. 5G) in human microglia presented a tendency to decrease upon exposure to ARPE-19 cell debris ($n = 5$). Pre-treatment with SCH58261 partially prevented these alterations ($n = 5$).

The blockade of $A_{2A}R$ in microglia prevents an inflammatory response and complement activation in ARPE-19 cells induced by exposure to microglia conditioned medium.

We have previously reported that the exposure of ARPE-19 cells to conditioned medium from reactive microglia increases the expression of pro-inflammatory markers⁹. In addition, we demonstrated that the blockade of $A_{2A}R$ prevents retinal inflammation^{24,25}. Therefore, we hypothesized that if $A_{2A}R$ blockade halts microglia reactivity, this would be sufficient to limit RPE responses to microglia-conditioned medium (MCM).

The mRNA expression of CCL2 and IL-8 (Fig. 6A and B) was up-regulated in ARPE-19 cells (2.98- and 11.7-fold increase comparing with the control MCM; $n = 6$) after exposure to MCM from Zymosan + PMA-treated cells. The incubation of ARPE-19 cells with cell culture supernatants from microglia pre-treated with $A_{2A}R$ antagonist before Zymosan + PMA exposure did not change the expression of CCL2 and IL-8, compared with the control.

The exposure of ARPE-19 cells to MCM from cells exposed to Zymosan + PMA increased the mRNA expression of CFB (2.15-fold increase relative to control MCM; $n = 6$; Fig. 6C) and downregulated CFH and CD55 mRNA expression (0.71- and 0.9-fold change, respectively; Fig. 6D and E), suggesting the activation of the

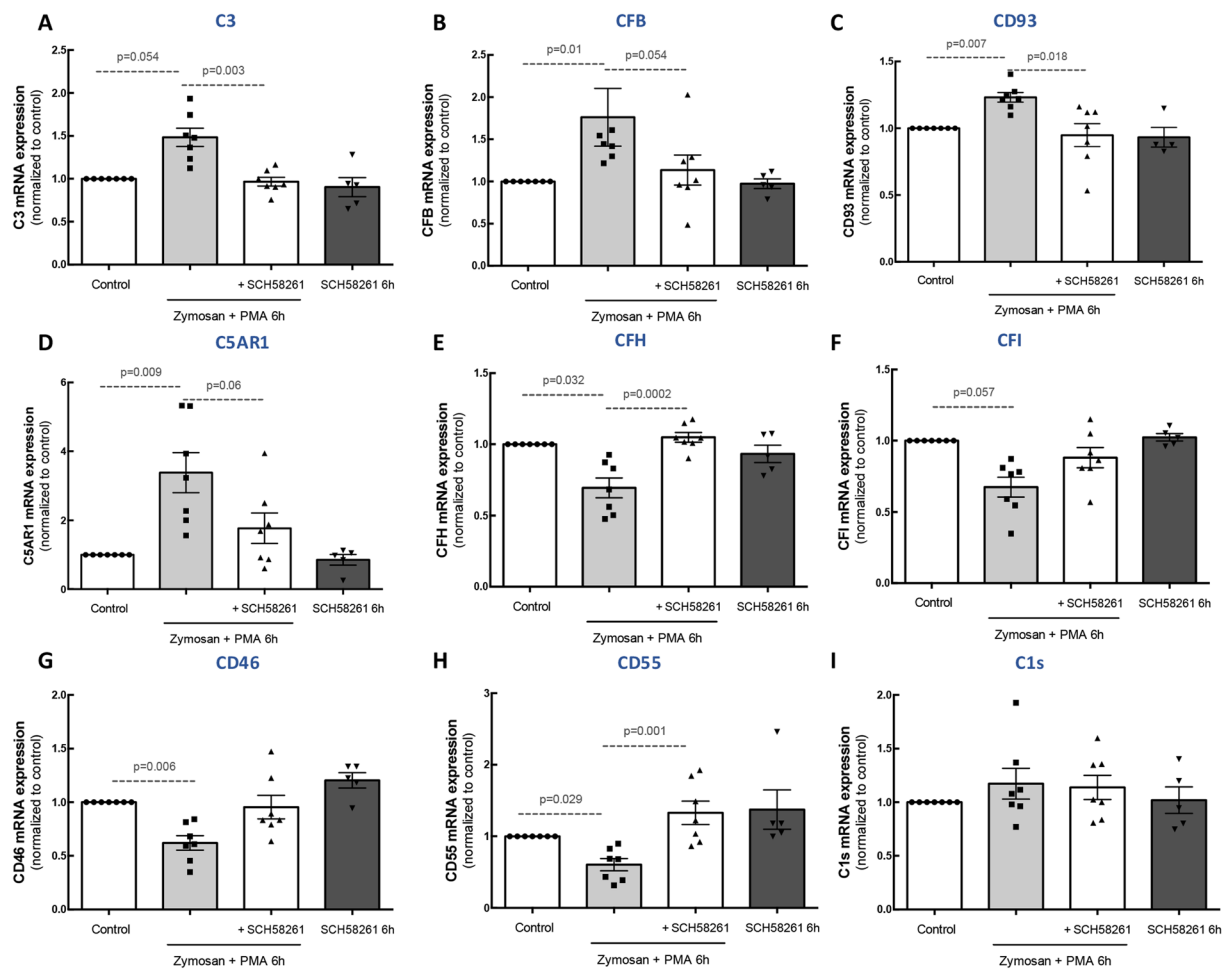


Figure 3. Blockade of $A_{2A}R$ prevents the alterations in complement cascade components in reactive human microglial cells. Human microglial cells were challenged with Zymosan + PMA in the presence or absence of 50 nM SCH58261. The expression levels of complement cascade components C3 (A), CFB (B), CFH (C), CFI (D), CD93 (E), C1s (F), C5AR1 (G), CD46 (H) and CD55 (I) were assessed by qPCR. Results are normalized to control and presented as the mean \pm SEM of 5–7 independent experiments (the individual data points for each condition are also presented). Kruskal-Wallis test, followed by Dunn's multiple comparison test.

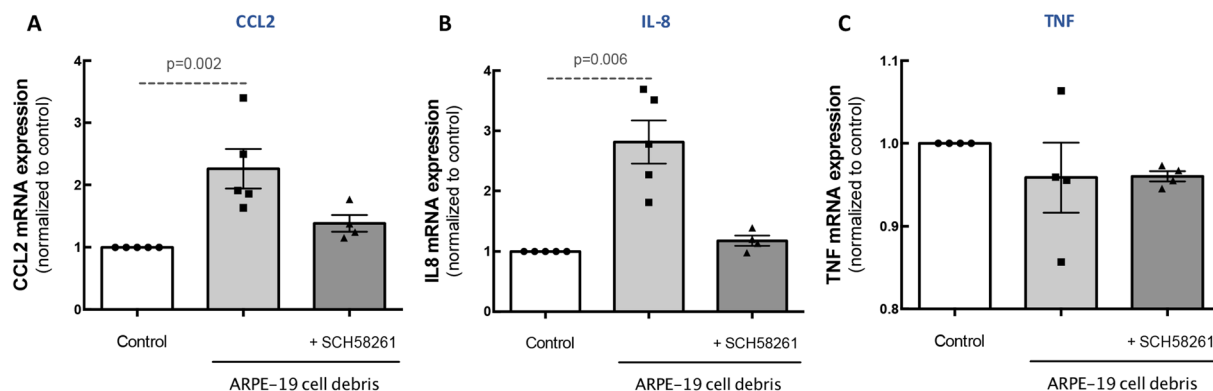


Figure 4. $A_{2A}R$ blockade prevents ARPE-19 debris-induced microglia inflammatory response. Human microglia were exposed to 5 μ g ARPE-19 apoptotic cell debris for 6 h in the absence or presence of the $A_{2A}R$ antagonist. The mRNA expression levels of CCL2 (A), TNF (B) and IL-8 (C) were assessed by qPCR. Results are normalized to control and presented as the mean \pm SEM of 5 independent experiments (the individual data points for each condition are also presented). Kruskal-Wallis test, followed by Dunn's multiple comparison test.

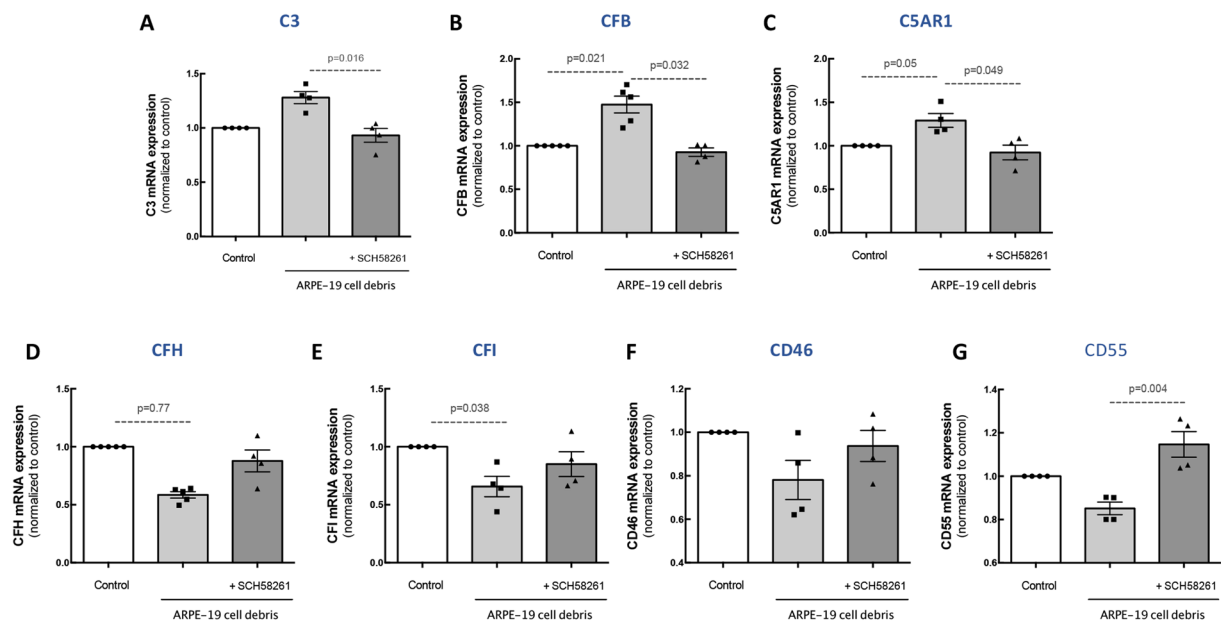


Figure 5. $A_{2A}R$ blockade prevents microglia complement cascade alterations induced by ARPE-19 debris. Human microglia were exposed to 5 $\mu\text{g}/\text{mL}$ ARPE-19 apoptotic cell debris for 6 h in the presence or absence of $A_{2A}R$ antagonist. The mRNA expression levels of complement cascade components C3 (A), CFB (B), CFH (C), CFI (D), C5AR1 (E), CD46 (F) and CD55 (G) were assessed by qPCR. Results are normalized to control and presented as the mean \pm SEM of 5 independent experiments (the individual data points for each condition are also presented). Kruskal-Wallis test, followed by Dunn's multiple comparison test.

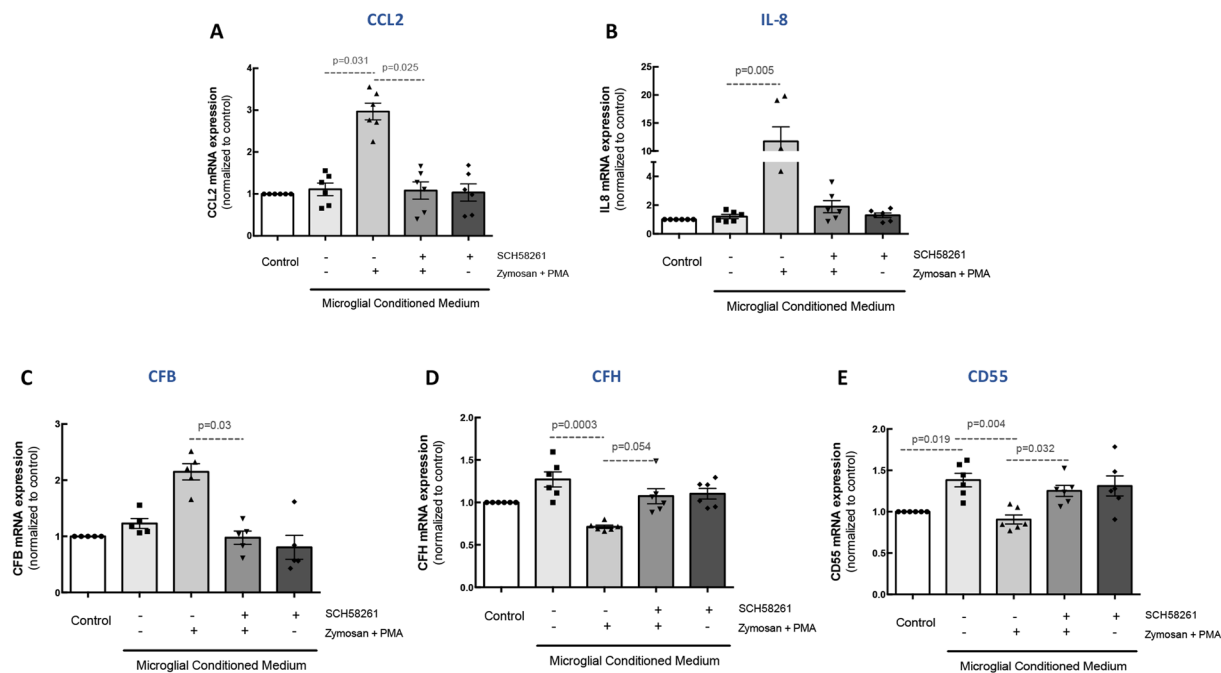


Figure 6. Blockade of $A_{2A}R$ in microglia prevents the inflammatory response and complement cascade alterations in ARPE-19 cells. Microglia were pretreated with 50 nM SCH58261 and then challenged with Zymosan + PMA for 6 h. MCM was added to ARPE-19 cells for 48 h. The mRNA expression of CCL2 (A) IL-8 (B), CFB (C), CFH (D), and CD55 (E) was assessed by qPCR. Results are normalized to control and presented as the mean \pm SEM of 6 independent experiments (the individual data points for each condition are also presented). Kruskal-Wallis test, followed by Dunn's multiple comparison test.

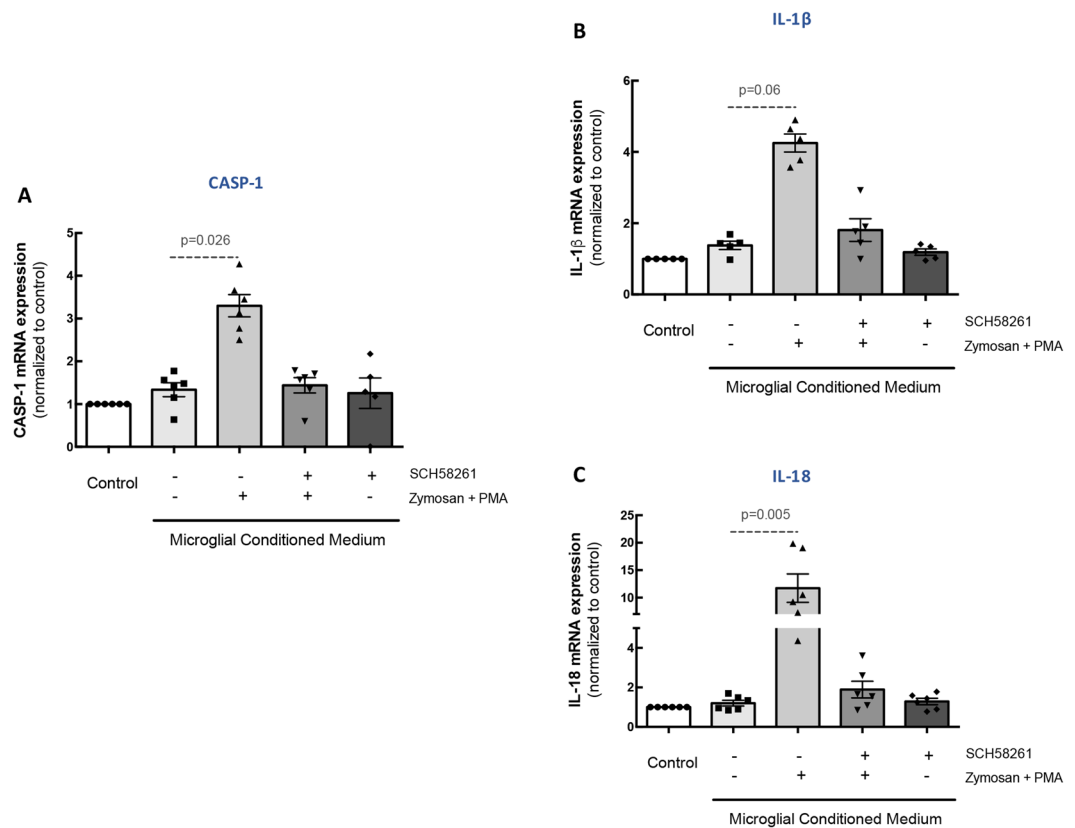


Figure 7. $A_{2A}R$ blockade in reactive human microglia prevents inflammasome activation in ARPE-19 cells. Microglia were pretreated with 50 nM SCH58261 and then challenged with Zymosan + PMA for 6 h. MCM was added to ARPE-19 cells for 48 h. The mRNA expression of caspase-1 (A) IL-1 β (B), and IL-18 (C) was assessed by qPCR. Results are normalized to control and presented as the mean \pm SEM of 6 independent experiments (the individual data points for each condition are also presented). Kruskal-Wallis test, followed by Dunn's multiple comparison test.

complement cascade in ARPE-19 cells. The $A_{2A}R$ blockade in microglial cells prevented the alterations in CFB, CFH, and CD55 detected in RPE cells. Also, MCM obtained from microglial cells exposed to SCH58261 did not alter the expression of these markers. In order to exclude a potential carryover effect, ARPE-19 cells were directly incubated with Zymosan + PMA, but no changes in the mRNA expression of these markers were detected (Supplementary Fig. 2). Importantly, ARPE-19 cells are not immunoreactive for $A_{2A}R$ (Supplementary Fig. 3) and do not express $A_{2A}R$ mRNA (data not shown).

$A_{2A}R$ blockade in microglia prevents inflammasome activation in RPE cells. We have recently described a role for reactive microglia in the activation of RPE inflammasome⁹. Therefore, we investigated whether blocking $A_{2A}R$ in microglia could prevent the activation of inflammasome in ARPE-19 cells triggered by exposure to MCM collected from microglia cultures exposed to pro-inflammatory conditions.

When ARPE-19 cells were exposed to MCM from non-stimulated microglial cell cultures, no significant alterations were detected in the expression of several components (caspase-1, IL-1 β and IL-18) of the inflammasome pathway components of ARPE-19 cells. However, in ARPE-19 cells exposed to MCM from microglial cell cultures exposed to Zymosan + PMA there was an up-regulation of the mRNA expression levels of caspase 1 (CASP1; Fig. 7A), IL-1 β (Fig. 7B) and IL-18 (Fig. 7C). Importantly, pre-treatment of human microglia with the $A_{2A}R$ antagonist prevented this effect (Fig. 7). MCM obtained from microglial cells exposed to SCH58261 did not alter the expression of these markers.

Blockade of $A_{2A}R$ increases microglia clearance of photoreceptor apoptotic debris. An effective phagocytic clearance of photoreceptor apoptotic debris by microglia is fundamental for the maintenance of retinal integrity^{30,31}. Hence, we next investigated the impact of $A_{2A}R$ blockade on the clearance of photoreceptor debris by microglia. For this purpose, control or Zymosan + PMA-treated human microglia, in the absence or presence of SCH58261, were exposed to the 661 W photoreceptor cell line apoptotic debris and the phagocytic efficiency was determined (Fig. 8A). Blockade of $A_{2A}R$ significantly increased the phagocytic efficiency of microglia ($137.8 \pm 6.1\%$ of non-treated, $n = 4$; Fig. 8B), suggesting an increase in the clearance of apoptotic material from photoreceptors.

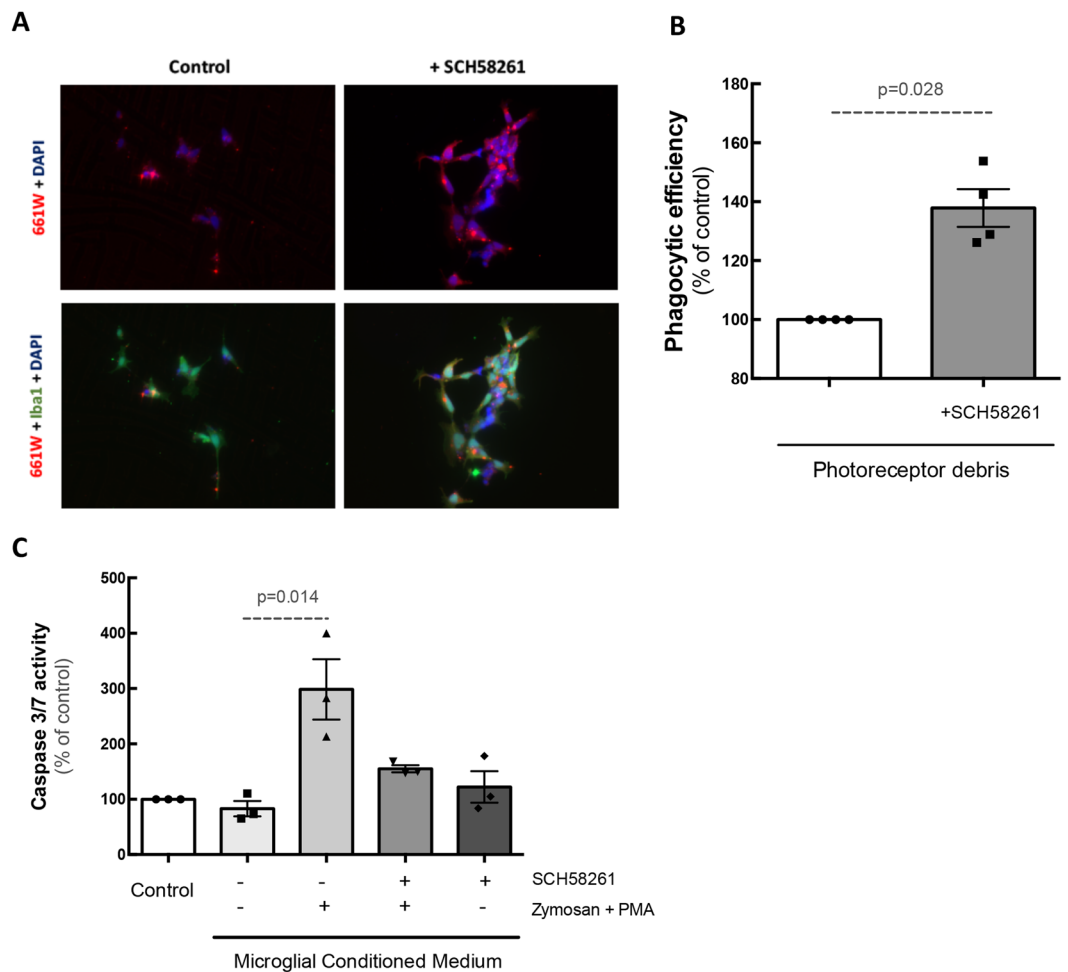


Figure 8. Blockade of $A_{2A}R$ increases the clearance of apoptotic photoreceptor debris by human microglial cells and prevents microglia-mediated increase of photoreceptor apoptosis. Human microglial cells (green) were exposed to CellTracker CM-DiI-labelled photoreceptors (red) in the absence or presence of SCH58261 for 6 h. Nuclei were counterstained with DAPI (blue). Representative images are depicted in (A) and the phagocytic efficiency was determined (B). Results are expressed as percentage of control and presented as the mean \pm SEM of 4 independent experiments (the individual data points for each condition are also presented). (C) Photoreceptors were exposed to microglia conditioned medium for 48 h and the activity of caspase 3/7 was determined. Results are expressed as percentage of control and presented as the mean \pm SEM of 3 independent experiments (the individual data points for each condition are also presented). Kruskal-Wallis test, followed by Dunn's multiple comparison test.

Control of microglia reactivity by the $A_{2A}R$ antagonist prevents 661W photoreceptor cell death. In order to further explore the influence of blocking $A_{2A}R$ on microglial-induced neurotoxicity, 661W photoreceptor-like cells were incubated for 48 h with untreated or Zymosan + PMA-treated MCM, in the absence or presence of SCH58261. Thereafter, the activity of caspases 3/7 was determined to estimate the apoptotic activity in 661W cells (Fig. 8C). 661W photoreceptors cultured with MCM from reactive cells showed increased caspase 3/7 activity ($289.5 \pm 54\%$ of the control, $n = 3$). The activity of caspase 3/7 was significantly reduced when microglia were pre-treated with SCH58261 ($115.6 \pm 6\%$ of control; $n = 3$), suggesting that the control of microglia reactivity due to $A_{2A}R$ blockade protects against the neurotoxic effects of microglia.

Discussion

In the present work, using *in vitro* models, we show for the first time that the blockade of $A_{2A}R$ in microglia impacts the expression of the complement system components in microglial cells. Importantly, the blockade of $A_{2A}R$ in microglia also reduces the inflammatory response in RPE cells, as well as the activation of the complement cascade and inflammasome. Likewise, blocking $A_{2A}R$ in microglia reduces photoreceptor cell death elicited by exposure to the supernatants of reactive microglia and increases the clearance of photoreceptor apoptotic material (Fig. 9).

Increased expression of $A_{2A}R$, as occurs in retinal microglia²⁴, has been associated with several CNS noxious conditions^{23,32}. It has been shown that activation of $A_{2A}R$ promotes microglia-mediated inflammatory responses, by potentiating NO release by activated microglia³³. Here, by exposing human microglial cells to Zymosan and

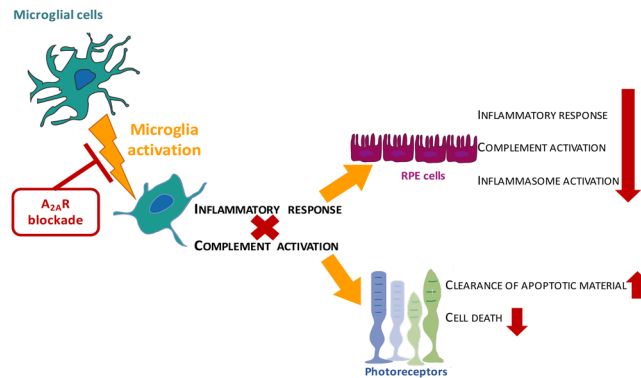


Figure 9. The blockade of $A_{2A}R$ in microglial cells prevent the loss of photoreceptors and reduced RPE dysfunction. Changes in homeostasis, trigger microglia reactivity that up-regulate inflammatory mediators and activate the complement cascade. This induce an inflammatory response is accompanied by complement and inflammasome activation on RPE cells and increased photoreceptor cell death. When microglial cells are treated with a selective antagonist of $A_{2A}R$, the microglial immune response is reduced (effects indicated with red symbols). Importantly, the blockade of $A_{2A}R$ in microglia reduces the inflammatory response in RPE cells, as well as the activation of the complement cascade and inflammasome. Likewise, blocking $A_{2A}R$ in microglia reduces photoreceptor cell death elicited by exposure to the supernatants of reactive microglia and increases the clearance of photoreceptor apoptotic material.

PMA, known to induce microglia activation by mimicking pathogenic infection^{28,34}, we report an increase in the concentration of extracellular adenosine as well as in the expression of $A_{2A}R$ in these cells, suggesting that $A_{2A}R$ signaling might be boosted in microglia thus promoting inflammation.

Parallel to what we have previously described for rat microglia²⁴, blockade of $A_{2A}R$ in human microglial cells prevents the reactive microglia phenotype, as indicated by the decrease in the expression of inflammatory mediators (CCL2, TNF and IL-8) and the reduced release of NO and phagocytic efficiency. Importantly, the exposure of human microglia to the apoptotic human ARPE-19 cell debris that resemble drusen material³⁵ also up-regulated the expression of inflammatory mediators (CCL2 and IL-8), which was also prevented by the blockade of $A_{2A}R$. Interestingly TNF expression was increased in microglia incubated with Zymosan + PMA but not with ARPE-19 debris, which suggests that different signaling pathways are elicited by the different noxious conditions. Several signaling pathways have been demonstrated to regulate TNF expression, such as nuclear factor kappa B (NF- κ B), as well as members of the mitogen activated protein kinase family, including ERK1/2 (extracellular receptor activated kinases 1/2), p38 and c-jun N-terminal kinase (JNK)³⁶. Future studies can focus on the signaling pathways activated in each condition.

Exposure of human microglia to an inflammatory stimulus or to ARPE-19 cell debris also induced the activation of the complement cascade by up-regulating the expression of C3, CFB, C1q and C5AR1 and down-regulating CFH, CFI, CD46 and CD93. Previous studies reported that the up-regulation of C3 in microglia is associated with the pathogenesis of age-related retinal diseases^{7,37,38}. Furthermore, when exposed to A2E, a drusen component, microglial cells up-regulate the expression of CFB and down-regulate the levels of CFH, a process that has been associated with photoreceptor loss⁸. Likewise, increased plasma levels and aqueous humor concentrations of complement components in AMD patients have been associated with low responsiveness to current therapies^{17,18}. Therefore, supplemental therapies targeting complement system activation have been suggested as novel strategies for AMD management^{17,29,39}. The selective antagonist of $A_{2A}R$ was able to prevent the alterations occurring in the complement system components in reactive human microglia, suggesting that $A_{2A}R$ not only modulates microglia pro-inflammatory responses, but can also modulate the activation of complement cascade.

Several studies have suggested a crosstalk between signals arising from reactive microglial cells and RPE that regulate the expression and secretion of pro-inflammatory, chemotactic, and pro-angiogenic molecules^{9,40,41}. This crosstalk may be also associated with drusen formation as a product of local inflammatory responses⁴². Here we show that reactive microglial cells may also trigger the activation of the complement system in ARPE-19 cells, further corroborating the role of microglia on RPE dysfunction. Again, the blockade of $A_{2A}R$ in microglia had the ability to prevent the activation of the complement system in RPE, suggesting that the control of microglia reactivity is sufficient to prevent microglia-induced effects on RPE.

NLRP3 inflammasome activation in the RPE has been described in AMD models^{21,43,44} and has been proposed to be a causal factor for RPE dysfunction and degeneration⁴⁵. In accordance with our recent report⁹, we detected increased expression of caspase-1, IL-1 β and IL-8 in ARPE-19 cells, supporting the idea that reactive microglial cells release factors that induce the activation of NLRP3 inflammasome in ARPE-19 cells. Remarkably, when microglial cells were treated with SCH58261, the activation of inflammasome in ARPE-19 was abolished, suggesting that the blockade of $A_{2A}R$ in microglia modulates inflammasome activation in RPE. In macrophages, adenosine modulates the inflammasome activation through $A_{2A}R$ ⁴⁶, which is in accordance with our data, where we found that blocking this receptor prevents the up-regulation of NLRP3 and IL-18 in reactive microglial cells (Supplementary Figure 4). However, there were no previous reports about the modulation of RPE inflammasome

by $A_{2A}R$. Also, we have previously described that reactive microglia-released material might induce activation of autophagy in RPE⁹. Although we have not evaluated the role of microglial $A_{2A}R$ blockade on the ARPE-19 autophagic pathways, one can speculate that autophagy might also be impacted, since autophagy regulates NLRP3 inflammasome activation^{47,48}. Indeed, future studies should focus on understanding a possible role of $A_{2A}R$ modulation in autophagy, which has been shown to have a fundamental role on the onset of AMD, as it modulates RPE inflammasome activation^{49–51} and RPE cell death^{52,53}.

Photoreceptor cell loss by apoptosis is a major feature of AMD⁵⁴, and an effective microglia-mediated clearance of the apoptotic cells is considered to be associated with an anti-inflammatory phenotype⁵⁵. Indeed, it has been shown that photoreceptor proteins are able to induce microglia phagocytic activity and promote the inflammatory response⁵⁶. Notably, the selective $A_{2A}R$ antagonist was able to increase the phagocytosis of photoreceptor debris by microglia, suggesting that blocking $A_{2A}R$ appears to have additional beneficial effects, such as increased clearance of the apoptotic material. Also, a more efficient clearance of the apoptotic material might contribute to a reduction of the inflammatory response triggered by the exposure to photoreceptor proteins. In this work we demonstrated that the $A_{2A}R$ antagonist reduces the phagocytosis of polystyrene beads by microglia, while it increased the phagocytosis of apoptotic cells. These apparent contradictory results operated by $A_{2A}R$ may imply molecular signals that induce distinct responses in microglia: it promotes the clearance of dead cells probably to halt the inflammatory response but when microglia face inert material, such as polystyrene beads, microglia phagocytose less when treated with SCH58261.

In fact, the crosstalk between microglial cells and photoreceptors is indubitable, since factors present in the culture medium of reactive microglial cells are able to induce photoreceptor cell apoptosis^{57–59}. Importantly, blockade of microglial $A_{2A}R$ is also able to reduce this outcome, suggesting that modulation of microglial cells reactivity by $A_{2A}R$ blockade can afford protective effects against photoreceptor cell death.

The role of inflammation and particularly the role of retinal microglia reactivity in the pathophysiology of AMD is unquestionable. Moreover, microglia-RPE crosstalk have long been associated with AMD pathogenesis, being speculated that this crosstalk can act as a positive feedback perpetuating the inflammatory response and sub-retinal microglia accumulation, fostering the proper mechanisms that promote AMD-related retinal dysfunction⁴⁰. Complement proteins^{8,37}, IL-1 β ⁶⁰ and NF- κ B^{10,57} have been already proposed as microglial modulatory factors that can in turn modulate the RPE inflammatory response being involved in photoreceptor loss. Still, novel therapeutic strategies aiming diminishing the effects of these mechanisms are required to reduce immune response in the context of AMD. Noteworthy, the control of the complement system has been identified as a possible therapeutic strategy for managing AMD²⁹, but some concerns might be raised relatively to its efficacy. Recently, ROCHE announced that the clinical trial (phase IIB) for Lampalizumab (NCT01602120), an antibody-binding fragment of a humanized monoclonal antibody that binds to complement factor D, which has been implicated in the pathogenesis of geographic atrophy⁶¹, did not reduced the geographic atrophy lesion area at 1 year of treatment⁶².

In this study, the different cell lines allowed us to dissect the role of $A_{2A}R$ blockade in microglial cells, the immune cells of the CNS, without the contribution of infiltrating immune cells, and the possible crosstalk between microglia, RPE cells and photoreceptors. Although it is important to refer that despite having some advantages over primary cells, cell lines have some limitations because they do not always accurately replicate the features of native cells in the tissue. Indeed, ARPE-19 cell line is one of the most commonly used cell lines for the study of RPE. However, these cells exhibit particularities different from RPE cells in their native environment, such as reduced transepithelial resistance, reduced levels of secreted cytokines, and different morphology^{63–65}. Despite the limitations of the cell lines, the present work paves the way to a better understanding on the role of microglial $A_{2A}R$ as a putative target for the treatment of AMD. Nevertheless, more studies are needed, using primary cultures and animal models of AMD to ascertain the therapeutic potential of $A_{2A}R$ antagonists.

In summary, in previous studies, we have suggested that selective $A_{2A}R$ blockade might be seen as a possible therapeutic strategy for glaucoma^{24–26,66}. In this work, using *in vitro* models, we show that an adequate modulation of microglial cell reactivity by blocking $A_{2A}R$ also presents beneficial effects on the modulation of the complement system, and might impact the microglia crosstalk with RPE and photoreceptors.

Methods

Cell lines and pharmacological compounds. The immortalized human microglia-SV40 cell line derived from primary human microglia was purchased from Applied Biological Materials, Inc. (ABM, Inc.). 661 W photoreceptor-like cells were a kind gift from Prof. Muayyad Al-Ubaidi (Department of Cell Biology, University of Oklahoma Health Sciences Center, Oklahoma City, OK, USA). ARPE-19 cells were obtained from ATCC (CRL-2302). Zymosan A from *Saccharomyces cerevisiae* and Phorbol 12-myristate 13-acetate (PMA) were purchased from Sigma-Aldrich. The $A_{2A}R$ antagonist SCH58261 was purchased from Merck Millipore.

Cell cultures and treatments. Human microglial cells were grown in collagen-coated T-75 cm² flasks and cultured in high glucose Dulbecco's modified Eagle's medium (DMEM) supplemented with 10% fetal bovine serum (FBS) and 1% penicillin/streptomycin, at 37 °C in a humidified atmosphere of 5% CO₂. Microglia were pretreated for 45 min with 50 nM SCH58261 ($A_{2A}R$ antagonist) and then challenged with Zymosan A (50 μ g/mL) and PMA (100 nM) for 6 h. For immunocytochemistry and assessment of mRNA expression, microglial cells were plated at a density of 1×10^4 cells and 1×10^5 cells/cm², respectively, in collagen-coated cover-slips on 12-well or 6-well plates (Fig. 10A).

Since drusen may result from cellular remnants and debris derived from degenerated RPE cells, debris obtained by serum-starved ARPE-19 cells were used to model the composition of drusen *in vitro*, as we reported previously⁹. To obtain RPE debris, ARPE-19 cells were starved by serum deprivation for 2 weeks, harvested,

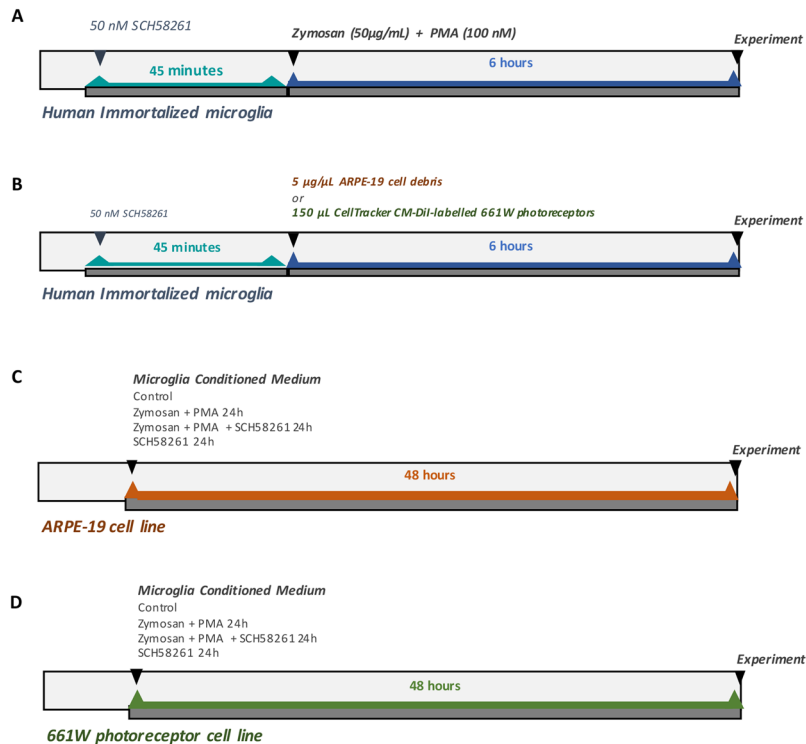


Figure 10. Schematic overview of the experimental design. **(A)** Human immortalized microglial cells were pretreated for 45 min with 50 nM SCH58261 ($A_{2A}R$ antagonist) and then challenged with Zymosan A (50 $\mu\text{g}/\text{mL}$) and PMA (100 nM) for 6 h. **(B)** Human immortalized microglial cells were challenged with 5 $\mu\text{g}/\mu\text{L}$ ARPE-19 cell debris for 6 h, previously untreated or treated with 50 nM SCH58261. **(C)** ARPE-19 cell line was cultured with MCM for 48 h. **(D)** 661 W photoreceptor cell line was cultured with MCM for 48 h.

centrifuged, and washed three times with PBS, and the pellet was frozen at -20°C . Microglial cells were incubated with 5 $\mu\text{g}/\mu\text{L}$ ARPE-19 cell debris for 6 h, previously treated or not with 50 nM SCH58261 (Fig. 10B).

ARPE-19 cell line was cultured in DMEM/F12 supplemented with 10% FBS and 1% penicillin/streptomycin. One day after seeding, the MCM was added to ARPE-19 cells for 48 h (Fig. 10C).

661 W photoreceptor cells were cultured in high glucose DMEM with L-glutamine, supplemented with 10% FBS and 1% penicillin/streptomycin, and maintained at 37°C in a humidified atmosphere of 5% CO_2 . One day after seeding, the MCM was added to 661 W cells for 48 h (Fig. 10D).

Adenosine quantification. The extracellular concentration of adenosine was quantified in human microglial cells supernatant using a fluorometric kit (BioVision), according to the instructions provided by the manufacturer.

Immunocytochemistry and image analysis. Cells were fixed with 4% formaldehyde, washed with PBS, and incubated in blocking buffer containing 10% goat serum and 0.3% Triton X-100. Subsequently, cells were incubated with the antibodies rabbit anti-Iba1 (1:150; Wako) or rabbit anti- $A_{2A}R$ (1:200; Thermo Scientific) in a solution containing 2.5% goat serum and 0.1% Triton X-100 for 1 h at room temperature. Cells were incubated with goat anti-rabbit Alexa 488 (A-11012, Life Technologies) or with 0.1 $\mu\text{g}/\text{ml}$ Phalloidin-TRITC (Sigma-Aldrich) (in the case of $A_{2A}R$ labeling). Cells were then washed with PBS and nuclei were stained with 4',6-diamidino-2-phenylindole (DAPI). Cover slips were mounted with fluorescent mounting medium (Dako), and fluorescence photomicrographs were taken with an AxioImager.M2 microscope (Carl Zeiss).

Densitometric analysis of $A_{2A}R$ staining was performed using ImageJ software (National Institutes of Health, Bethesda, MD, USA) and mean grey value was calculated as previously described²⁵, with the formula:

$$\text{CTCF} = \text{Integrated density} - (\text{area of selected cell} \times \text{mean fluorescence of background reading})$$

Real-time quantitative Polymerase Chain Reaction (PCR). Total RNA was extracted from human microglial cells or ARPE-19 using the NucleoSpin[®] RNA Mini Kit (Macherey-Nagel), according to the manufacturer's instructions. RNA was quantified spectrophotometrically using a NanoDrop 2000 (Thermo Scientific) and then stored at -80°C . Amplification of cDNA was with RevertAid[™] H Minus First strand cDNA Synthesis Kit (Thermo Scientific), according to the instructions provided by the manufacturer, using 1 μg of total RNA.

Gene	Primer Forward	Primer Reverse	Roche UPL probe numbers
Hprt	5'-tgacctgattatttgcatacc-3'	5'-cgagcaagacgttcagtcct-3'	73
Adora2A	5'-tgaccctacattgccatc-3'	5'-tccaacctagcatgggagtc-3'	3
Ccl2	5'-agtctctgccgacctct-3'	5'-gtgactggggcattgattg-3'	40
TNF	5'-cagcctcttctctctgat-3'	5'-gccagaggctgattagaga-3'	29
IL-8	5'-agacagcagagcacacaagc-3'	5'-cacagtggatggctctcc-3'	72
C3	5'-ccactggaggtgtctgacg-3'	5'-ctggtacaggcggatctct-3'	1
CFB	5'-tccactgctatgacggttaca-3'	5'-gctgtctgccactccat-3'	53
CD93	5'-ggccatggagaaccagtaca-3'	5'-ggaatggggagttcaaacg-3'	83
C5AR1	5'-ggaggaccttcgatcctc-3'	5'-gggggtataattgaaggagt-3'	54
CFH	5'-gaatgggttctcttaacca-3'	5'-cctcctgtaaggtaaaagtacca-3'	80
CFI	5'-tggaccaagataagacaatgtca-3'	5'-acctcttggatcagcaccct-3'	78
CD46	5'-cgtaagccccaatagt-3'	5'-acttactaaagggtgtttcca-3'	10
CD55	5'-ctgctggtctgttgc-3'	5'-tcctcgggaaaactgtacg-3'	20
C1s	5'-cttgcgagagaagatttga-3'	5'-ggaccaattgccgatcctc-3'	38
CASP-1	5'-ccaggacattaaaaaaggaaactgta-3'	5'-ccaaaaacctttacagaaggatcctc-3'	4
IL-18	5'-aacaactatttctgcaggaat-3'	5'-tgccacaaagtgtgcaat-3'	46
IL-1 β	5'-tacctgtcctcgtgtttaa-3'	5'-tctttgggtaattttgggatc-3'	78
NLRP3	5'-aaagatgagccgaagtgg-3'	5'-atccactctctcaatgctg-3'	72

Table 1. Primers used in qPCR and RT-PCR.

Amplification of 50 ng cDNA was conducted in an ABI7900HT machine (Applied Biosystems) in 10 μ l reaction mixtures containing 1 \times TaqMan Universal PCR Master Mix (Applied Biosystems), 200 nM of primers, and 0.125 μ l of dual-labeled UPL probe (Roche Applied Science). The reaction parameters were as follows: 2 min 50 $^{\circ}$ C hold, 30 min 60 $^{\circ}$ C hold, and 5 min 95 $^{\circ}$ C hold, followed by 45 cycles of 20 s 94 $^{\circ}$ C melt and 1 min 60 $^{\circ}$ C anneal/extension. Primer sequences and UPL probe numbers are listed on Table 1. Ct values were converted to “relative quantification” using the $2^{-\Delta\Delta Ct}$ method, using the method described by Livak⁶⁷. *Hprt* was used as housekeeping gene.

Nitrite measurement. Nitric oxide concentration was estimated in the supernatant of human microglial cells by quantifying the concentration of nitrites using the Griess reaction method (Promega), as previously described and according to the manufacturer’s instructions. The results are presented as percentage of control.

Microparticles phagocytosis assay. After plating and overnight seeding, microglial cells were treated as described above and 2 h after incubated with 2 μ l of micro-particles based on polystyrene solutions (Sigma-Aldrich) for 6 h. After washing 3 times with PBS, 5 images were randomly acquired for each condition under an inverted microscope (Carl Zeiss). Phagocytic efficiency was calculated as described previously²⁴. Results are presented as percentage of control.

661W apoptotic material phagocytosis assay. 661 W photoreceptor cells were starved by serum deprivation and harvested and fluorescently labeled using CellTracker CM-DiI (Invitrogen, Carlsbad, CA, USA). Human microglial phagocytic efficiency was assessed as previously described⁵⁹. Briefly, microglial cells were treated with 150 μ l of apoptotic 661W-labeled solution for 6 h in the presence or absence of SCH58261 (50 nM) (Fig. 10B). Cells were then fixed with 4% formaldehyde and immunolabeled with an antibody rabbit anti-Iba1 (1:150; Wako)⁶⁸, as described above. Preparations were observed with an inverted fluorescence microscope Axiomager.M2 microscope (Carl Zeiss) and from each experimental condition, at least 5 fields were randomly acquired. Phagocytic efficiency was determined using the formula previously described²⁴. Results are presented as percentage of control.

661 W photoreceptor apoptosis assay. Microglia-induced neurotoxicity was investigated as previously described⁵⁹. Briefly, 661 W photoreceptor cells were incubated for 48 h with culture supernatants from control-, Zymosan + PMA-, Zymosan + PMA + SCH58261-, or SCH58261-treated microglial cells. Apoptotic cell death was determined using the Caspase-Glo[®] 3/7 Assay (Promega), according to the manufacturer’s instructions. Relative luciferase units (RLUs) reflect the level of apoptotic cell death. Results are presented as percentage of control.

Statistical analysis. Normality of the data was assessed with Shapiro-Wilk normality test. Since data did not follow a Gaussian distribution, all data was analyzed using non-parametric tests: Mann-Whitney test (for comparison of two groups) or Kruskal-Wallis test (when comparing more than two groups), followed by Dunn’s multiple comparison correction test, as indicated in the figure legends. The values of P are presented above the bars for each comparison. The results are presented as mean \pm standard error of the mean (SEM) and the individual data points are also shown. Values of P < 0.05 were considered statistically significant. The statistical analysis was performed in Prism 7.0 Software for Mac OS X (GraphPad Software, Inc).

References

- Wong, W. L. *et al.* Global prevalence of age-related macular degeneration and disease burden projection for 2020 and 2040: a systematic review and meta-analysis. *Lancet Glob Health* **2**, e106–116, [https://doi.org/10.1016/S2214-109X\(13\)70145-1](https://doi.org/10.1016/S2214-109X(13)70145-1) (2014).
- Wong, T. Y. *et al.* The natural history and prognosis of neovascular age-related macular degeneration: a systematic review of the literature and meta-analysis. *Ophthalmology* **115**, 116–126, <https://doi.org/10.1016/j.ophtha.2007.03.008> (2008).
- Kauppinen, A., Paterno, J. J., Blasiak, J., Salminen, A. & Kaarniranta, K. Inflammation and its role in age-related macular degeneration. *Cell Mol Life Sci* **73**, 1765–1786, <https://doi.org/10.1007/s00018-016-2147-8> (2016).
- Chen, M. & Xu, H. Parainflammation, chronic inflammation, and age-related macular degeneration. *J Leukoc Biol* **98**, 713–725, <https://doi.org/10.1189/jlb.3RJ0615-239R> (2015).
- Madeira, M. H., Boia, R., Santos, P. F., Ambrosio, A. F. & Santiago, A. R. Contribution of microglia-mediated neuroinflammation to retinal degenerative diseases. *Mediators Inflamm* **2015**, 673090, <https://doi.org/10.1155/2015/673090> (2015).
- Karlstetter, M. *et al.* Retinal microglia: just bystander or target for therapy? *Prog Retin Eye Res* **45**, 30–57, <https://doi.org/10.1016/j.preteyeres.2014.11.004> (2015).
- Rutar, M. *et al.* Analysis of complement expression in light-induced retinal degeneration: synthesis and deposition of C3 by microglia/macrophages is associated with focal photoreceptor degeneration. *Invest Ophthalmol Vis Sci* **52**, 5347–5358, <https://doi.org/10.1167/iovs.10-7119> (2011).
- Ma, W., Coon, S., Zhao, L., Fariss, R. N. & Wong, W. T. A2E accumulation influences retinal microglial activation and complement regulation. *Neurobiol Aging* **34**, 943–960, <https://doi.org/10.1016/j.neurobiolaging.2012.06.010> (2013).
- Nebel, C., Aslanidis, A., Rashid, K. & Langmann, T. Activated microglia trigger inflammasome activation and lysosomal destabilization in human RPE cells. *Biochem Biophys Res Commun* **484**, 681–686, <https://doi.org/10.1016/j.bbrc.2017.01.176> (2017).
- Zhang, C. *et al.* Activation of microglia and chemokines in light-induced retinal degeneration. *Mol Vis* **11**, 887–895 (2005).
- Wagner, E. & Frank, M. M. Therapeutic potential of complement modulation. *Nat Rev Drug Discov* **9**, 43–56, <https://doi.org/10.1038/nrd3011> (2010).
- Orsini, F., De Blasio, D., Zangari, R., Zanier, E. R. & De Simoni, M. G. Versatility of the complement system in neuroinflammation, neurodegeneration and brain homeostasis. *Front Cell Neurosci* **8**, 380, <https://doi.org/10.3389/fncel.2014.00380> (2014).
- Cipriani, V. *et al.* Genetic variation in complement regulators and susceptibility to age-related macular degeneration. *Immunobiology* **217**, 158–161, <https://doi.org/10.1016/j.imbio.2011.09.002> (2012).
- Fritsche, L. G. *et al.* A large genome-wide association study of age-related macular degeneration highlights contributions of rare and common variants. *Nat Genet* **48**, 134–143, <https://doi.org/10.1038/ng.3448> (2016).
- Wu, L. *et al.* Association between polymorphisms of complement pathway genes and age-related macular degeneration in a Chinese population. *Invest Ophthalmol Vis Sci* **54**, 170–174, <https://doi.org/10.1167/iovs.12-10453> (2013).
- Black, J. R. & Clark, S. J. Age-related macular degeneration: genome-wide association studies to translation. *Genet Med* **18**, 283–289, <https://doi.org/10.1038/gim.2015.70> (2016).
- Lechner, J. *et al.* Higher plasma levels of complement C3a, C4a and C5a increase the risk of subretinal fibrosis in neovascular age-related macular degeneration: Complement activation in AMD. *Immun Ageing* **13**, 4, <https://doi.org/10.1186/s12979-016-0060-5> (2016).
- Schick, T. *et al.* Local complement activation in aqueous humor in patients with age-related macular degeneration. *Eye (Lond)* **31**, 810–813, <https://doi.org/10.1038/eye.2016.328> (2017).
- Franchi, L., Eigenbrod, T., Munoz-Planillo, R. & Nunez, G. The inflammasome: a caspase-1-activation platform that regulates immune responses and disease pathogenesis. *Nat Immunol* **10**, 241–247, <https://doi.org/10.1038/ni.1703> (2009).
- Celkova, L. & Doyle, S. L. & Campbell, M. NLRP3 Inflammasome and Pathobiology in AMD. *J Clin Med* **4**, 172–192, <https://doi.org/10.3390/jcm4010172> (2015).
- Tseng, W. A. *et al.* NLRP3 inflammasome activation in retinal pigment epithelial cells by lysosomal destabilization: implications for age-related macular degeneration. *Invest Ophthalmol Vis Sci* **54**, 110–120, <https://doi.org/10.1167/iovs.12-10655> (2013).
- Brandstetter, C., Patt, J., Holz, F. G. & Krohne, T. U. Inflammasome priming increases retinal pigment epithelial cell susceptibility to lipofuscin phototoxicity by changing the cell death mechanism from apoptosis to pyroptosis. *J Photochem Photobiol B* **161**, 177–183, <https://doi.org/10.1016/j.jphotobiol.2016.05.018> (2016).
- Santiago, A. R. *et al.* Role of microglia adenosine A(2A) receptors in retinal and brain neurodegenerative diseases. *Mediators Inflamm* **2014**, 465694, <https://doi.org/10.1155/2014/465694> (2014).
- Madeira, M. H. *et al.* Selective A2A receptor antagonist prevents microglia-mediated neuroinflammation and protects retinal ganglion cells from high intraocular pressure-induced transient ischemic injury. *Transl Res* **169**, 112–128, <https://doi.org/10.1016/j.trsl.2015.11.005> (2016).
- Madeira, M. H. *et al.* Adenosine A2AR blockade prevents neuroinflammation-induced death of retinal ganglion cells caused by elevated pressure. *J Neuroinflammation* **12**, 115, <https://doi.org/10.1186/s12974-015-0333-5> (2015).
- Boia, R. *et al.* Treatment with A2A receptor antagonist KW6002 and caffeine intake regulate microglia reactivity and protect retina against transient ischemic damage. *Cell Death Dis* **8**, e3065, <https://doi.org/10.1038/cddis.2017.451> (2017).
- Cunha, R. A. How does adenosine control neuronal dysfunction and neurodegeneration? *J Neurochem* **139**, 1019–1055, <https://doi.org/10.1111/jnc.13724> (2016).
- Harrigan, T. J., Abdullaev, I. F., Jour'd'heil, D. & Mongin, A. A. Activation of microglia with zymosan promotes excitatory amino acid release via volume-regulated anion channels: the role of NADPH oxidases. *J Neurochem* **106**, 2449–2462, <https://doi.org/10.1111/j.1471-4159.2008.05553.x> (2008).
- Xu, H. & Chen, M. Targeting the complement system for the management of retinal inflammatory and degenerative diseases. *Eur J Pharmacol* **787**, 94–104, <https://doi.org/10.1016/j.ejphar.2016.03.001> (2016).
- Wolf, S. A., Boddeke, H. W. & Kettenmann, H. Microglia in Physiology and Disease. *Annu Rev Physiol* **79**, 619–643, <https://doi.org/10.1146/annurev-physiol-022516-034406> (2017).
- Kim, S. Y. Retinal phagocytes in age-related macular degeneration. *Macrophage (Houst)* **2**, <https://doi.org/10.14800/macrophage.698> (2015).
- Yu, L. *et al.* Adenosine A2A receptor antagonists exert motor and neuroprotective effects by distinct cellular mechanisms. *Ann Neurol* **63**, 338–346, <https://doi.org/10.1002/ana.21313> (2008).
- Saura, J. *et al.* Adenosine A2A receptor stimulation potentiates nitric oxide release by activated microglia. *J Neurochem* **95**, 919–929, <https://doi.org/10.1111/j.1471-4159.2005.03395.x> (2005).
- Smith, M. E., van der Maesen, K., Somera, F. P. & Sobel, R. A. Effects of phorbol myristate acetate (PMA) on functions of macrophages and microglia *in vitro*. *Neurochem Res* **23**, 427–434 (1998).
- Karlstetter, M. *et al.* Polysialic acid blocks mononuclear phagocyte reactivity, inhibits complement activation, and protects from vascular damage in the retina. *EMBO Mol Med* **9**, 154–166, <https://doi.org/10.15252/emmm.201606627> (2017).
- Sweet, M. J. & Hume, D. A. Endotoxin signal transduction in macrophages. *J Leukoc Biol* **60**, 8–26 (1996).
- Natoli, R. *et al.* Retinal Macrophages Synthesize C3 and Activate Complement in AMD and in Models of Focal Retinal Degeneration. *Invest Ophthalmol Vis Sci* **58**, 2977–2990, <https://doi.org/10.1167/iovs.17-21672> (2017).
- Rutar, M., Valter, K., Natoli, R. & Provis, J. M. Synthesis and propagation of complement C3 by microglia/monocytes in the aging retina. *PLoS One* **9**, e93343, <https://doi.org/10.1371/journal.pone.0093343> (2014).

39. Nozaki, M. *et al.* Drusen complement components C3a and C5a promote choroidal neovascularization. *Proc Natl Acad Sci USA* **103**, 2328–2333, <https://doi.org/10.1073/pnas.0408835103> (2006).
40. Ma, W., Zhao, L., Fontainhas, A. M., Fariss, R. N. & Wong, W. T. Microglia in the mouse retina alter the structure and function of retinal pigmented epithelial cells: a potential cellular interaction relevant to AMD. *PLoS One* **4**, e7945, <https://doi.org/10.1371/journal.pone.0007945> (2009).
41. Anderson, D. H. *et al.* The pivotal role of the complement system in aging and age-related macular degeneration: hypothesis revisited. *Prog Retin Eye Res* **29**, 95–112, <https://doi.org/10.1016/j.preteyeres.2009.11.003> (2010).
42. Zhou, J., Jang, Y. P., Kim, S. R. & Sparrow, J. R. Complement activation by photooxidation products of A2E, a lipofuscin constituent of the retinal pigment epithelium. *Proc Natl Acad Sci USA* **103**, 16182–16187, <https://doi.org/10.1073/pnas.0604255103> (2006).
43. Wang, Y. *et al.* NLRP3 Upregulation in Retinal Pigment Epithelium in Age-Related Macular Degeneration. *Int J Mol Sci* **17**, <https://doi.org/10.3390/ijms17010073> (2016).
44. Brandstetter, C., Mohr, L. K., Latz, E., Holz, F. G. & Krohne, T. U. Light induces NLRP3 inflammasome activation in retinal pigment epithelial cells via lipofuscin-mediated photooxidative damage. *J Mol Med (Berl)* **93**, 905–916, <https://doi.org/10.1007/s00109-015-1275-1> (2015).
45. Gao, J. *et al.* NLRP3 inflammasome: activation and regulation in age-related macular degeneration. *Mediators Inflamm* **2015**, 690243, <https://doi.org/10.1155/2015/690243> (2015).
46. Ouyang, X. *et al.* Adenosine is required for sustained inflammasome activation via the A(2)A receptor and the HIF-1 α pathway. *Nat Commun* **4**, 2909, <https://doi.org/10.1038/ncomms3909> (2013).
47. Zhong, Z., Sanchez-Lopez, E. & Karin, M. Autophagy, NLRP3 inflammasome and auto-inflammatory/immune diseases. *Clin Exp Rheumatol* **34**, 12–16 (2016).
48. Nakahira, K. *et al.* Autophagy proteins regulate innate immune responses by inhibiting the release of mitochondrial DNA mediated by the NALP3 inflammasome. *Nat Immunol* **12**, 222–230, <https://doi.org/10.1038/ni.1980> (2011).
49. Phippo, N. *et al.* Decline in cellular clearance systems induces inflammasome signaling in human ARPE-19 cells. *Biochim Biophys Acta* **1843**, 3038–3046, <https://doi.org/10.1016/j.bbamcr.2014.09.015> (2014).
50. Iannaccone, A. *et al.* Circulating Autoantibodies in Age-Related Macular Degeneration Recognize Human Macular Tissue Antigens Implicated in Autophagy, Immunomodulation, and Protection from Oxidative Stress and Apoptosis. *PLoS One* **10**, e0145323, <https://doi.org/10.1371/journal.pone.0145323> (2015).
51. Iannaccone, A. *et al.* Retinal pigment epithelium and microglia express the CD5 antigen-like protein, a novel autoantigen in age-related macular degeneration. *Exp Eye Res* **155**, 64–74, <https://doi.org/10.1016/j.exer.2016.12.006> (2017).
52. Kaarniranta, K., Tokarz, P., Koskela, A., Paterno, J. & Blasiak, J. Autophagy regulates death of retinal pigment epithelium cells in age-related macular degeneration. *Cell Biol Toxicol* **33**, 113–128, <https://doi.org/10.1007/s10565-016-9371-8> (2017).
53. Yao, J. *et al.* Deletion of autophagy inducer RB1CC1 results in degeneration of the retinal pigment epithelium. *Autophagy* **11**, 939–953, <https://doi.org/10.1080/15548627.2015.1041699> (2015).
54. Dunaief, J. L., Dentechev, T., Ying, G. S. & Milam, A. H. The role of apoptosis in age-related macular degeneration. *Arch Ophthalmol* **120**, 1435–1442 (2002).
55. Sierra, A., Abiega, O., Shahraz, A. & Neumann, H. Janus-faced microglia: beneficial and detrimental consequences of microglial phagocytosis. *Front Cell Neurosci* **7**, 6, <https://doi.org/10.3389/fncel.2013.00006> (2013).
56. Kohno, H. *et al.* Photoreceptor proteins initiate microglial activation via Toll-like receptor 4 in retinal degeneration mediated by all-trans-retinal. *J Biol Chem* **288**, 15326–15341, <https://doi.org/10.1074/jbc.M112.448712> (2013).
57. Yang, L. P., Zhu, X. A. & Tso, M. O. A possible mechanism of microglia-photoreceptor crosstalk. *Mol Vis* **13**, 2048–2057 (2007).
58. Karlstetter, M. *et al.* Translocator protein (18 kDa) (TSPO) is expressed in reactive retinal microglia and modulates microglial inflammation and phagocytosis. *J Neuroinflammation* **11**, 3, <https://doi.org/10.1186/1742-2094-11-3> (2014).
59. Aslanidis, A. *et al.* Activated microglia/macrophage whey acidic protein (AMWAP) inhibits NF κ B signaling and induces a neuroprotective phenotype in microglia. *J Neuroinflammation* **12**, 77, <https://doi.org/10.1186/s12974-015-0296-6> (2015).
60. Natoli, R. *et al.* Microglia-derived IL-1 β promotes chemokine expression by Muller cells and RPE in focal retinal degeneration. *Mol Neurodegener* **12**, 31, <https://doi.org/10.1186/s13024-017-0175-y> (2017).
61. Katschke, K. J. Jr. *et al.* Inhibiting alternative pathway complement activation by targeting the factor D exosite. *J Biol Chem* **287**, 12886–12892, <https://doi.org/10.1074/jbc.M112.345082> (2012).
62. Roche, F. H.-L. *ROCHE - Investor update - media release (Accessed October 25, 2017)*, <https://www.roche.com/dam/jcr:a3969247-3a45-4501-8940-306fbd1dc97f/en/med-cor-2017-09-08b.pdf> (2017).
63. Ablonczy, Z. *et al.* Human retinal pigment epithelium cells as functional models for the RPE *in vivo*. *Invest Ophthalmol Vis Sci* **52**, 8614–8620, <https://doi.org/10.1167/iovs.11-8021> (2011).
64. Dunn, K. C. *et al.* Use of the ARPE-19 cell line as a model of RPE polarity: basolateral secretion of FGF5. *Invest Ophthalmol Vis Sci* **39**, 2744–2749 (1998).
65. Fronk, A. H. & Vargis, E. Methods for culturing retinal pigment epithelial cells: a review of current protocols and future recommendations. *J Tissue Eng* **7**, 2041731416650838, <https://doi.org/10.1177/2041731416650838> (2016).
66. Madeira, M. H. *et al.* Caffeine administration prevents retinal neuroinflammation and loss of retinal ganglion cells in an animal model of glaucoma. *Sci Rep* **6**, 27532, <https://doi.org/10.1038/srep27532> (2016).
67. Livak, K. J. & Schmittgen, T. D. Analysis of relative gene expression data using real-time quantitative PCR and the 2^{-Delta Delta} C(T) Method. *Methods* **25**, 402–408, <https://doi.org/10.1006/meth.2001.1262> (2001).
68. Luckoff, A., Scholz, R., Sennlaub, F., Xu, H. & Langmann, T. Comprehensive analysis of mouse retinal mononuclear phagocytes. *Nat Protoc* **12**, 1136–1150, <https://doi.org/10.1038/nprot.2017.032> (2017).

Acknowledgements

M.H. Madeira was a recipient of a short-term fellowship from the Federation of European Biochemical Societies (FEBS). The work was supported by DFG research unit FOR2240 (Lymph) Angiogenesis and cellular immunity in inflammatory diseases of the eye, Foundation for Science and Technology (PEst UID/NEU/04539/2013), COMPETE-FEDER (POCI-01-0145-FEDER-007440), and Centro 2020 Regional Operational Program (CENTRO-01-0145-FEDER-000008: BrainHealth 2020).

Author Contributions

M.H.M., K.R., A.R.S. and T.L. conceived and designed the experiments. M.H.M. performed the experiments. M.H.M., K.R., A.F.A., A.R.S. and T.L. analyzed the data. A.F.A., A.R.S. and T.L. contributed with reagents/materials/analysis tools. M.H.M., K.R., A.F.A., A.R.S. and T.L. wrote the paper. All contributing authors have read and approved the final version of the manuscript.

Additional Information

Supplementary information accompanies this paper at <https://doi.org/10.1038/s41598-018-20733-2>.

Competing Interests: The authors declare that they have no competing interests.

Publisher's note: Springer Nature remains neutral with regard to jurisdictional claims in published maps and institutional affiliations.



Open Access This article is licensed under a Creative Commons Attribution 4.0 International License, which permits use, sharing, adaptation, distribution and reproduction in any medium or format, as long as you give appropriate credit to the original author(s) and the source, provide a link to the Creative Commons license, and indicate if changes were made. The images or other third party material in this article are included in the article's Creative Commons license, unless indicated otherwise in a credit line to the material. If material is not included in the article's Creative Commons license and your intended use is not permitted by statutory regulation or exceeds the permitted use, you will need to obtain permission directly from the copyright holder. To view a copy of this license, visit <http://creativecommons.org/licenses/by/4.0/>.

© The Author(s) 2018